

PROCEEDINGS OF SPIE

SPIDigitalLibrary.org/conference-proceedings-of-spie

Characterization of Redlen CZT detectors for hard x-ray astronomy

Sean N. Pike, Fiona A. Harrison, Jill A. Burnham, Walter Cook, Brian W. Grefenstette, et al.

Sean N. Pike, Fiona A. Harrison, Jill A. Burnham, Walter Cook, Brian W. Grefenstette, Kristin K. Madsen, Hiromasa Miyasaka, Julian M. Sanders, Andrew A. Sosanya, "Characterization of Redlen CZT detectors for hard x-ray astronomy," Proc. SPIE 10762, Hard X-Ray, Gamma-Ray, and Neutron Detector Physics XX, 1076214 (13 September 2018); doi: 10.1117/12.2321990

SPIE.

Event: SPIE Optical Engineering + Applications, 2018, San Diego, California, United States

Characterization of Redlen CZT detectors for hard X-ray astronomy

Sean N. Pike, Fiona A. Harrison, Jill A. Burnham, Walter Cook, Brian W. Grefenstette, Kristin K. Madsen, Hiromasa Miyasaka, Julian M. Sanders, and Andrew A. Sosanya

Space Radiation Laboratory, California Institute of Technology, Pasadena, CA, 91125

ABSTRACT

We present the results of ongoing characterization of Cadmium Zinc Telluride (CZT) semiconductors produced by Redlen Technologies. In particular we hope to determine their viability for future X-ray astronomy missions such as the *High Energy X-ray Probe (HEX-P)*. The fully fabricated hybrid detectors consist of CZT crystals with a collecting area of $2\text{ cm} \times 2\text{ cm}$ and thickness of 3 mm mounted on a custom pixelated ASIC originally designed for the *Nuclear Spectroscopic Telescope Array (NuSTAR)* mission, which launched in 2012. We present the results of inter-pixel conductance and leakage current tests as well as spectral characterization using an ^{241}Am source. Although further calibration and testing is necessary to determine the capabilities of these detectors, preliminary results indicate that Redlen CZT will be able to achieve spectral resolution and noise levels comparable to those of the CZT detectors currently in use aboard *NuSTAR*.

Keywords: CZT, Redlen Technologies, X-ray detectors, *NuSTAR*, astronomy

1. INTRODUCTION

Cadmium Zinc Telluride (CZT) detectors are used in a wide range of applications, and have been of particular utility to the astronomy and astrophysics community. The material is well-suited for detection of hard X-rays and gamma-rays thanks to the high atomic numbers of its constitutive elements.¹ Astronomical missions which have utilized CZT detectors include the Burst Alert Telescope (BAT) instrument on the *Neil Gehrels Swift Observatory*², which makes use of a coded-aperture mask in combination with an array of CZT detectors in order to detect and localize gamma-ray bursts (GRBs) and the Cadmium-Zinc-Telluride Imager³ (CZTI) on *AstroSat*⁴ which observes GRBs and other transients using of a plane of CZT detectors with both a coded-aperture mask and a set of tantalum collimators.

The *Nuclear Spectroscopic Telescope Array (NuSTAR)*⁵ observes the X-ray sky in the 3-79 keV band with two focal plane modules, each containing four CZT detectors. Each $2\text{ cm} \times 2\text{ cm} \times 2\text{ mm}$ crystal is mated to a custom pixelated ASIC via a flip-chip bonding process to produce a “hybrid.” The 32×32 pixelated design of the *NuSTAR* hybrid allows the instrument to take advantage of the small-pixel effect.⁶ This results in improved energy resolution by minimizing the signal induced by positively-charged holes which are created when a region of the detector is ionized by an incoming photon. This pixelated design also means that each pixel can be manually activated or deactivated, making operation of the instrument more flexible. Because the readout electronics provide the time, location, and energy of each interacting photon, the scientific applications are wide-ranging. However, the pixelated architecture is not without disadvantages. For example, when charge is split between adjacent pixels, energy resolution is degraded.

This pixelated architecture, in addition to other technologies, will be inherited by the *High Energy X-ray Probe (HEX-P)*.⁷ This mission concept will achieve improved spatial and energy resolution in addition to an observable bandpass from 2 keV extending as far as 200 keV. While *NuSTAR* was launched with CZT detectors from eV Products, we are currently testing Cadmium Telluride (CdTe) detectors from AcroRad Co. and CZT detectors from Redlen Technologies for use in this and other future missions. Low inter-pixel conductance, which minimizes charge sharing between adjacent pixels, low noise in the form of leakage current, and good spectral resolution are all necessary for a detector to produce scientifically useful data. Crystal uniformity is also

Send correspondences to S.N.P.: spike@caltech.edu

prioritized, and material from a given vendor should be relatively consistent in quality in order to reduce the time and monetary costs of testing, calibrating, and ultimately flying detectors. In this paper, we present the initial results of our ongoing characterization of CZT detectors from Redlen Technologies. This paper may be considered a continuation of the work we presented in Pike et al. (2018).⁸ While those results were incomplete due to high electronic noise introduced during fabrication, the detectors presented here do not appear to be affected by the same problem.

2. DATA AND RESULTS

We have performed several tests using two Redlen CZT crystals (hereafter Redlen 1 and Redlen 2) with dimensions $2\text{ cm} \times 2\text{ cm} \times 3\text{ mm}$, each attached to a *NuSTAR* ASIC via the same flip-chip bonding procedure which was used to produce the hybrids aboard *NuSTAR*. Below, we present the methods and results of these tests. We have measured the inter-pixel conductance (Section 2.1) and leakage current (Section 2.2) of both detectors, and we have conducted preliminary spectral characterization of the second detector, Redlen 2 (Section 2.3). In addition to presenting the results of these tests, we compare the results to similar measurements of detectors currently aboard *NuSTAR*. In order to compare the spectra measured by different detectors, we applied a simple pixel-by-pixel gain correction wherein we determined the position in channels of the 60 keV line emitted by a ^{241}Am source as measured by each pixel. Thus we are able to determine the eV/channel gain value for each pixel and convert measurements into units of energy. Rather than compare the Redlen hybrids to the fully calibrated *NuSTAR* hybrids, we apply the same method to both datasets in order to make a more reasonable comparison. Note that this is still not a perfect comparison, in part because the detectors have different thicknesses, and that further corrections are needed to determine whether Redlen detectors can achieve the same or better energy resolution as their *NuSTAR* counterparts.

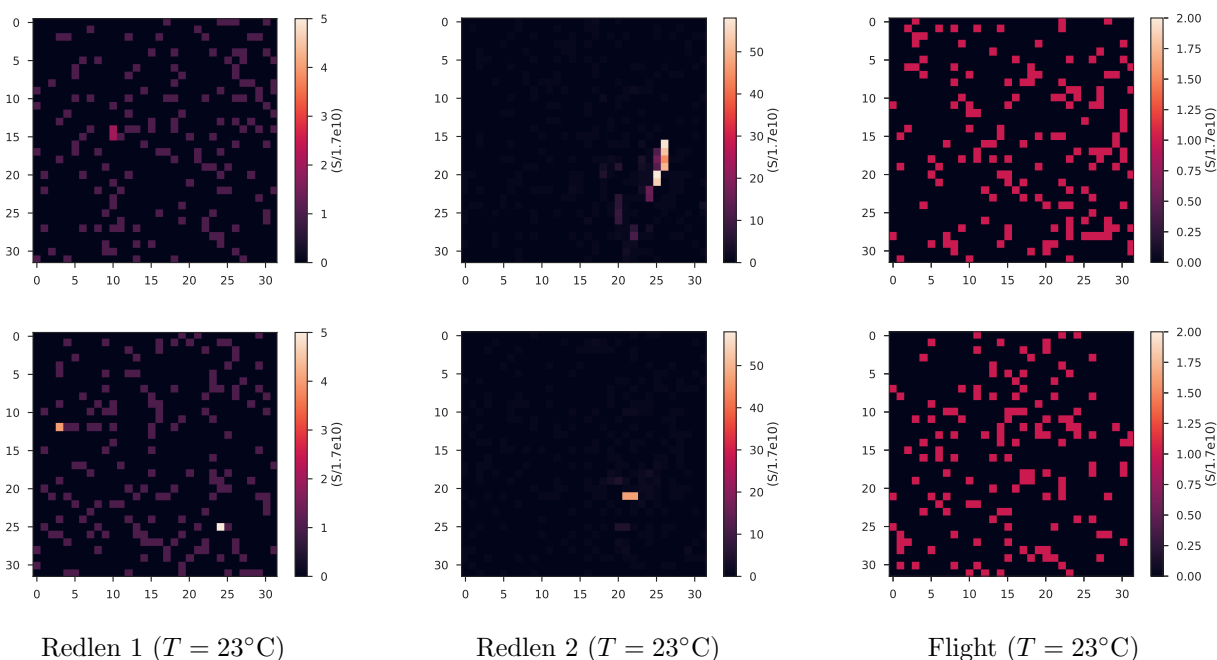


Figure 1. Results of inter-pixel conductance measurements for two Redlen hybrids and one flight hybrid. Due to the experimental setup, each hybrid produces two conductance scans: one in the vertical direction, shown in the top row, and one in the horizontal, shown in the bottom row. The conductance for both Redlen detectors is generally low, but a small region of Redlen 2 exhibits much higher conductance. It is currently unclear whether this is a property of the CZT material or a result of the fabrication process.

2.1 Inter-pixel Conductance

An important property of CZT detectors is the extent to which the charge is shared across adjacent pixels. Charge-sharing results in more difficult calibration as well as loss of spectral resolution. As such, inter-pixel conductance should be minimized. Due to the design of the *NuSTAR* hybrid, we are unable to directly probe the conductance between any given pair of adjacent pixels. Instead, we can determine the conductance across a given pixel (i.e. between a pair of pixels separated by another pixel) in either the horizontal or vertical direction. Thus, we scan each row of pixels and determine the conductance across the pixels of that row. We then similarly scan each column. The result is two sets of conductance values for each pixel. We performed inter-pixel conductance scans for the two Redlen hybrids at room temperature ($\sim 23^\circ\text{C}$).

The Redlen hybrids exhibit low conductance between pixels in both the horizontal and vertical directions, as is shown in Figure 1. The conductance of most pixels is of the order 10^{-10} S, however there are pixels which exhibit higher conductance. In particular, Redlen 2 contains a region of ~ 20 pixels which exhibit conductance an order of magnitude higher than the rest of the detector. Further measurements are necessary to determine whether this feature may be attributed to the Redlen CZT or to a flaw in the hybridization process. Nonetheless, Redlen 1 shows uniformity and low conductance which are very similar to those measured for the *NuSTAR* hybrid.

2.2 Leakage Current

We next investigated the leakage current of the Redlen hybrids. Leakage current is defined as the current through the detector which results from applying a bias voltage. We measured the leakage current through each pixel at several bias voltages between 100 V and 600 V, and operating temperatures between -10°C and 23°C . In Figure 2 we present results of the leakage current measurements at a bias voltage of 500 V and $T = 5^\circ\text{C}$.

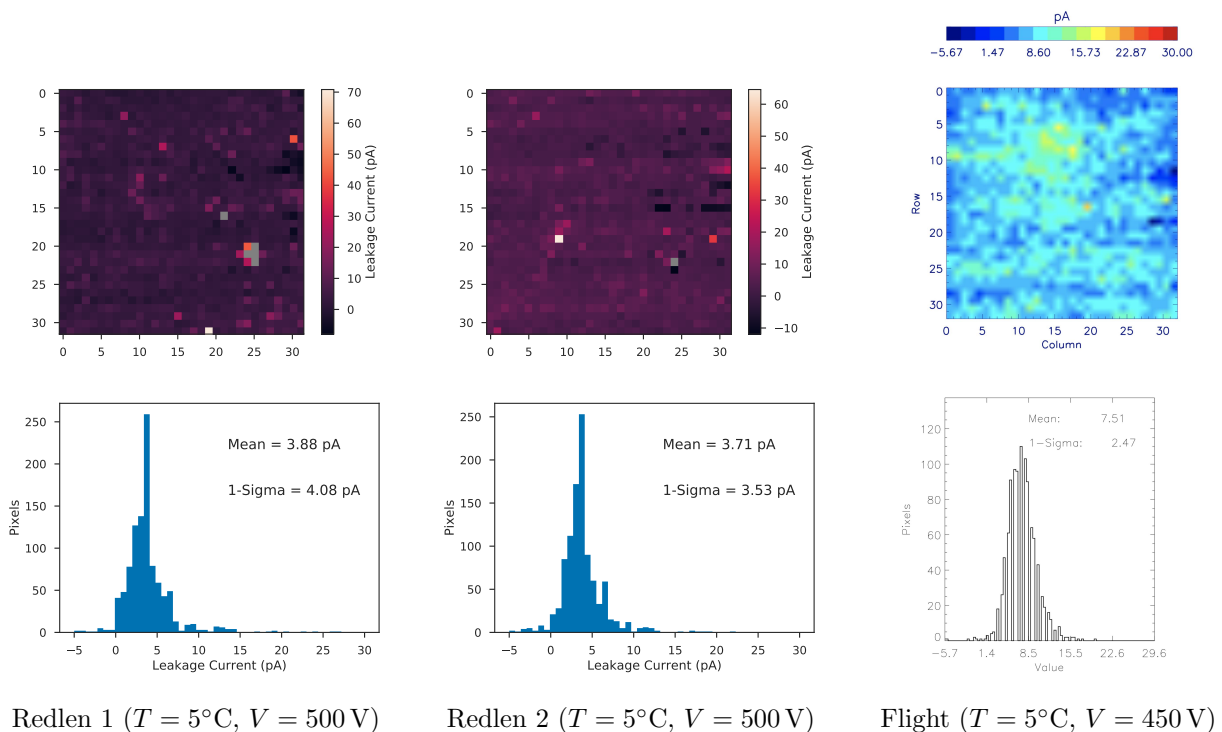


Figure 2. Results of pixel-by-pixel leakage current measurements for two Redlen hybrids and one flight hybrid. The top row of figures shows the leakage current for each pixel. Pixels shown in gray exhibit leakage current greater than 75 pA. The bottom row shows the distribution of leakage current measurements for each hybrid. The Redlen hybrids exhibit lower mean leakage current than the flight hybrid, but show more variance between pixels.

We find that the Redlen hybrids exhibit a lower mean leakage current than the flight hybrids at similar operating conditions. A lower leakage current is to be expected for a thicker detector, but the improvement by nearly a factor of 2 exceeds expectations for an increased thickness by a factor of 1.5. In addition, the leakage current is uniform across the Redlen hybrids. However the variance across pixels is larger than that of the flight hybrid, with standard deviations comparable to the mean. In contrast, the leakage current measured in the flight hybrids exhibits less spread with a standard deviation of around one third of the mean and around half of the standard deviation measured in the Redlen hybrids. In addition, we find that at high voltages (> 400 V), a small number of pixels begin to exhibit anomalously high leakage current (> 40 pA at 5°C). While this increases the noise at high voltage, thanks to the design of the *NuSTAR* ASIC we are able to turn off individual pixels so that operation at high voltage is feasible. This allows us to benefit from improved energy resolution at high voltage while minimizing adverse effects.

2.3 Spectral Characterization

Finally, we have measured the spectrum of a ^{241}Am source using one of the Redlen hybrids (Redlen 2). A bias voltage of 500 V was applied across the detector, while a Temptronic Thermostream device was used to maintain an operating temperature of 5°C . In order to determine the spectral resolution of the detectors, we determined the width of the 60 keV line for each hybrid after applying the channel-to-energy gain correction to each pixel. We have also applied identical corrections to an analogous dataset collected using a flight hybrid in order to compare to the Redlen hybrid.

The results of this experiment are shown in Figure 3. We find that with the preliminary gain correction described in Section 1, a FWHM of around 1.2 keV at 60 keV (2%) is achieved with the Redlen hybrid. Although this is slightly worse than the FWHM of 1.0 keV achieved during a similar test with a *NuSTAR* hybrid, this is

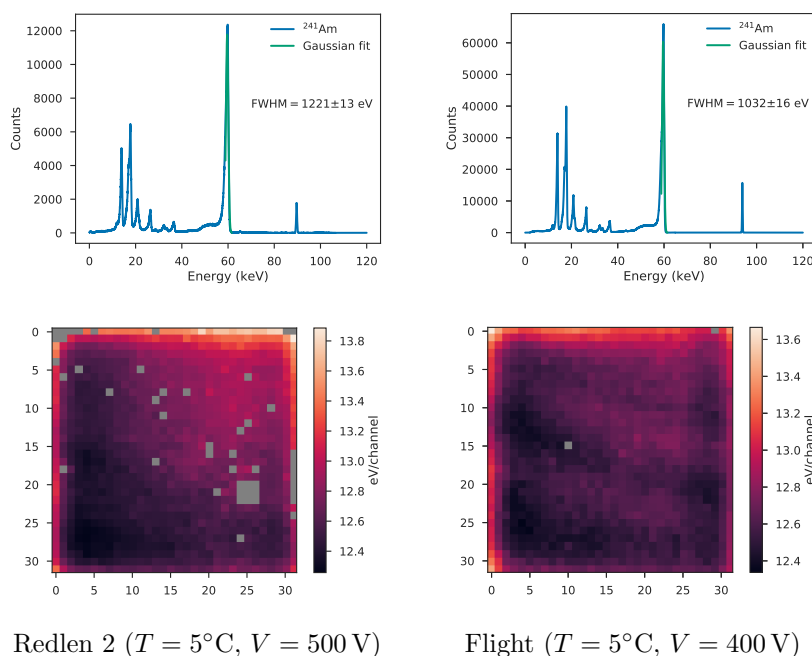


Figure 3. Results of irradiating Redlen hybrid 2 and a flight detector with an ^{241}Am source. The top row of figures shows the gain corrected spectra. The 60 keV line has been fitted to a Gaussian, shown in green, to determine the width of the line as measured by each hybrid. The small line between 90 keV and 100 keV is due to an artificial pulse applied to the pixel at position (10, 10). The width of this line is an indication of the electronic noise. The bottom row of figures shows the pixel-by-pixel gain for each hybrid as determined by measuring the position of the 60 keV line by each pixel. Pixels shown in gray were either turned off during testing due to a high number of spurious events or did not produce a spectrum suitable for an accurate gain measurement.

meant as a loose comparison rather than a final conclusion regarding the differences between these detectors. As such, this spectral resolution is a good indicator that the Redlen material can achieve similar measurement capabilities to those of the *NuSTAR* detectors. In order to fully characterize the spectral resolution, however, further corrections, such as depth-of-interaction and charge sharing corrections, should be applied.

In addition to the spectral resolution, the eV/channel values for each pixel are shown in Figure 3. The gain properties are very similar to those of the *NuSTAR* hybrid, with values varying between 12 and 14 eV/channel. In addition to this, both the Redlen and *NuSTAR* hybrids show uniformity in their per-pixel gain values, with only slight gradients visible in the gain maps. It should be noted that a significant number of pixels (shown in gray in Figure 3) were either turned off during testing due to high noise or did not produce a spectrum which allowed for reasonable fitting of the 60 keV line and so do not have a corresponding gain measurement. The cause of both of these behaviors is still under investigation.

3. DISCUSSION AND CONCLUSIONS

We have performed several tests of the material properties and detector capabilities of two Redlen CZT detectors. By mating these detectors to custom pixelated *NuSTAR* ASICs, we are able to determine how the crystal properties vary from pixel to pixel, and we can compare to hybrids which are currently being used to collect scientific data aboard *NuSTAR*. Thus we can begin to probe the usefulness of Redlen CZT for future astronomical missions.

In measurements of inter-pixel conductivity, the Redlen material performs well in general, with conductivity comparable to that of the CZT detectors aboard *NuSTAR*. However, in one of the Redlen hybrids, we observe a region of high conductivity. It is still unclear whether this non-uniformity is due to the Redlen material or to other factors introduced during hybridization. Leakage current measurements provide a separate probe of crystal uniformity, under which the Redlen CZT performs well. There is little sign of non-uniformity across both Redlen detectors, and the mean leakage current is lower than that of the *NuSTAR* hybrids under similar conditions, due in part to the Redlen detectors' increased thickness. Finally, we have irradiated one of the Redlen detectors with a ^{241}Am source. We find that the eV/channel gain is uniform across the detector and that the spectral resolution is comparable to that achieved by *NuSTAR* hybrids under similar conditions.

Taking these results as a whole, we are able to conclude that the Redlen detectors which we have investigated exhibit spatial uniformity which is comparable to the *NuSTAR* detectors, with some exceptions such as a small region of high conductance. In addition, we can expect low noise and limited charge-sharing effects. The spectral resolution achieved in preliminary tests indicate that this is the case, as the resolution is not significantly worse than the thinner *NuSTAR* detectors. Finally, the spectral resolution will only improve upon more thorough calibration and corrections. Charge sharing effects can also be probed directly by measuring the proportion of events which are spread over multiple pixels. Although there remain open questions, our initial results suggest that Redlen CZT material may prove viable for use in future astronomical missions.

ACKNOWLEDGMENTS

This work was supported under NASA grant NNX13AC55G.

REFERENCES

- [1] Eisen, Y. and Shor, A., "CdTe and CdZnTe materials for room-temperature X-ray and gamma ray detectors," *Journal of Crystal Growth* **184-185**, 1302–1312 (1998).
- [2] Barthelmy, S. D., "The Burst Alert Telescope (BAT) on the Swift MIDEX mission," *Proceedings of SPIE - The International Society for Optical Engineering* **5165**, 175–189 (2004).
- [3] Bhalerao, V., Bhattacharya, D., Vibhute, A., Pawar, P., Rao, A. R., Hingar, M. K., Khanna, R., Kutty, A. P., Malkar, J. P., Patil, M. H., Arora, Y. K., Sinha, S., Priya, P., Samuel, E., Sreekumar, S., Vinod, P., Mithun, N. P., Vadawale, S. V., Vagshette, N., Navalgund, K. H., Sarma, K. S., Pandiyan, R., Seetha, S., and Subbarao, K., "The Cadmium Zinc Telluride Imager on AstroSat," *Journal of Astrophysics and Astronomy* **38**(2) (2017).

- [4] Singh, K. P., Tandon, S. N., Agrawal, P. C., Antia, H. M., Manchanda, R. K., Yadav, J. S., Seetha, S., Ramadevi, M. C., Rao, A. R., Bhattacharya, D., Paul, B., Sreekumar, P., Bhattacharyya, S., Stewart, G. C., Hutchings, J., Annapurni, S. A., Ghosh, S. K., Murthy, J., Pati, A., Rao, N. K., Stalin, C. S., Girish, V., Sankarasubramanian, K., Vadawale, S., Bhalerao, V. B., Dewangan, G. C., Dedhia, D. K., Hingar, M. K., Katoch, T. B., Kothare, A. T., Mirza, I., Mukerjee, K., Shah, H., Shah, P., Mohan, R., Sangal, A. K., Nagabhusana, S., Sriram, S., Malkar, J. P., Sreekumar, S., Abbey, A. F., Hansford, G. M., Beardmore, A. P., Sharma, M. R., Murthy, S., Kulkarni, R., Meena, G., Babu, V. C., and Postma, J., “ASTROSAT mission,” in [*Proceedings of SPIE*], **9144** (2014).
- [5] Harrison, F. A., Craig, W. W., Christensen, F. E., Hailey, C. J., Zhang, W. W., Boggs, S. E., Stern, D., Cook, W. R., Forster, K., Giommi, P., Grefenstette, B. W., Kim, Y., Kitaguchi, T., Koglin, J. E., Madsen, K. K., Mao, P. H., Miyasaka, H., Mori, K., Perri, M., Pivovarov, M. J., Puccetti, S., Rana, V. R., Westergaard, N. J., Willis, J., Zoglauer, A., An, H., Bachetti, M., Barriere, N. M., Bellm, E. C., Bhalerao, V., Brejnholt, N. F., Fuerst, F., Liebe, C. C., Markwardt, C. B., Nynka, M., Vogel, J. K., Walton, D. J., Wik, D. R., Alexander, D. M., Cominsky, L. R., Hornschemeier, A. E., Hornstrup, A., Kaspi, V. M., Madejski, G. M., Matt, G., Molendi, S., Smith, D. M., Tomsick, J. a., Ajello, M., Ballantyne, D. R., Balokovic, M., Barret, D., Bauer, F. E., Blandford, R. D., Brandt, W. N., Brenneman, L. W., Chiang, J., Chakrabarty, D., Chenevez, J., Comastri, A., Elvis, M., Fabian, A. C., Farrah, D., Fryer, C. L., Gotthelf, E. V., Grindlay, J. E., Helfand, D. J., Krivonos, R., Meier, D. L., Miller, J. M., Natalucci, L., Ogle, P., Ofek, E. O., Ptak, A., Reynolds, S. P., Rigby, J. R., Tagliaferri, G., Thorsett, S. E., Treister, E., and Urry, C. M., “The Nuclear Spectroscopic Telescope Array (NuSTAR) Mission,” *The Astrophysical Journal* **770**(1), 20 (2013).
- [6] Zumbiehl, A., Hage-Ali, M., Fougeres, P., Koebel, J. M., Regal, R., Rit, C., Ayoub, M., and Siffert, P., “Modelling and 3D optimisation of CdTe pixels detector array geometry - Extension to small pixels,” *Nuclear Instruments and Methods in Physics Research, Section A: Accelerators, Spectrometers, Detectors and Associated Equipment* **469**(2), 227–239 (2001).
- [7] Harrison, F. A., Madsen, K. K., Grefenstette, B. W., Stern, D. K., Hornschemeier, A. E., Boggs, S. E., Brandt, N., Brenneman, L., Chakrabarty, D., Christensen, F. E., Craig, W., Fabian, A. C., Elvis, M., Grindlay, J., Hailey, C., Hornstrup, A., Kaspi, V., Madjeski, G., Matt, G., Miller, J. M., Miyasaka, H., Molendi, S., Zhang, W. W., Tomsick, J., and Yukita, M., “The high-energy x-ray probe (HEX-P),” in [*SPIE Astronomical Telescopes and Instrumentation*], (2018).
- [8] Pike, S. N., Harrison, F. A., Burnham, J. A., Cook, W. W., Grefenstette, B. W., Madsen, K. K., and Miyasaka, H., “Characterizing Redden CZT detectors for X-ray astronomy,” in [*SPIE 10709, High Energy, Optical, and Infrared Detectors for Astronomy VIII*], (2018).